Available online at www.sciencedirect.com
ScienceDirect
Journal of Solid State Chemistry 181 (2008) 1273–1278
JOURNAL OF SOLID STATE CHEMISTRY
www.elsevier.com/locate/jssc

Rapid Communication

High pressure synthesis and structure of a new magnetoplumbite-type cobalt oxide $SrCo_{12}O_{19}$

Shintaro Ishiwata[a,*], Ichiro Terasaki[a], Masaki Azuma[b], Mikio Takano[b]

[a]Department of Applied Physics, Waseda University, Ookubo, Shinjuku, Tokyo 169-8555, Japan
[b]Institute for Chemical Research, Kyoto University, Gokashou, Uji 611-0011, Japan

Received 8 December 2007; received in revised form 15 February 2008; accepted 20 February 2008
Available online 29 February 2008

Abstract

A new magnetoplumbite-type hexagonal cobalt oxide, $SrCo_{12}O_{19}$, has been synthesized at a high pressure of 3 GPa and its structural and magnetic properties have been studied using single crystalline samples. Bond-valence calculations for five crystallographically independent Co sites show a rather wide charge distribution from +2.15 to +3.50. Magnetic measurements have revealed anisotropic magnetic behavior below a magnetic ordering temperature of 80 K. Comparative discussions on the structure–property relationship for $SrCo_{12}O_{19}$ and related compounds suggest the presence of localized spins with a uniaxial anisotropy at the trigonal bipyramidal site.

Keywords: High pressure synthesis; Cobalt oxides; Magnetoplumbite; $SrCo_6O_{11}$

1. Introduction

Magnetoplumbite-type (M-type) hexagonal ferrites $AFe_{12}O_{19}$ (A = La, Sr, Ba, Pb) are widely used permanent magnetic materials. Due to their strong uniaxial anisotropy along the hexagonal axis, large saturation magnetization, and low cost, they have been utilized in the form of nano particles for perpendicular magnetic recording [1,2]. In addition, a number of M-type oxides without Fe ions are also reported. Typical examples are $AAl_{12}O_{19}$ (A = Ca, Sr) known as hosts of laser and luminescent materials [3], and $SrCr_8Ga_4O_{19}$, of which magnetism has been studied from the viewpoint of spin frustration on a Kagomé lattice [4]. Then, it is presumable that Co will build up of the M-type structure because it is a spinel-forming metal as well as Fe and Al [5]. However, while Co^{2+}-containing M-type hexaferrites such as $BaFe_{12-2x}Co_xTi_xO_{19}$ ($0<x\leqslant 6$) have been synthesized to improve their magnetic performance [6–8], a completely Co-substituted compound has not been reported yet.

Recently, a new R-type hexagonal cobalt oxide $SrCo_6O_{11}$ has been discovered by a high-pressure (HP) technique [9]. This material has a uniaxial magnetization similar to the M-type hexaferrites but shows metallic behavior unlike them [10]. Below the magnetic ordering temperature (T_m~20 K), the magnetization curves measured along the hexagonal axis show a $\frac{1}{3}$ plateau prior to the $\frac{3}{3}$ saturation, which reflects the nature of the frustrated Ising-like spins. In addition, a strong coupling between the magnetism and electronic conduction shows up as a giant two-staged magnetoresistance [11]. Since the M-type compounds consist of an alternate stacking of the R-type ($SrCo_6O_{11}$) and the spinel (S)-type ($2Co_3O_4$) blocks as shown in Fig. 1(b), the remarkable magnetoelectronic properties discovered in $SrCo_6O_{11}$ spurred us to try HP syntheses of the M-type hexagonal cobalt oxide $SrCo_{12}O_{19}$.

2. Experimental

$SrCo_{12}O_{19}$ was prepared with a conventional cubic anvil-type HP apparatus. For polycrystalline samples, γ-Na_xCoO_2 (x~0.5) and $SrCl_2$ mixed in a molar ratio of 1:1 were used as the starting materials. The mixture was sealed in a gold capsule and was subjected to a treatment at 3 GPa

*Corresponding author. Present address: Cross-Correlated Materials Research Group (CMRG), FRS, RIKEN, Wako 351-0198, Japan.
E-mail address: ishiwata@riken.jp (S. Ishiwata).

0022-4596/$ - see front matter © 2008 Elsevier Inc. All rights reserved.
doi:10.1016/j.jssc.2008.02.024

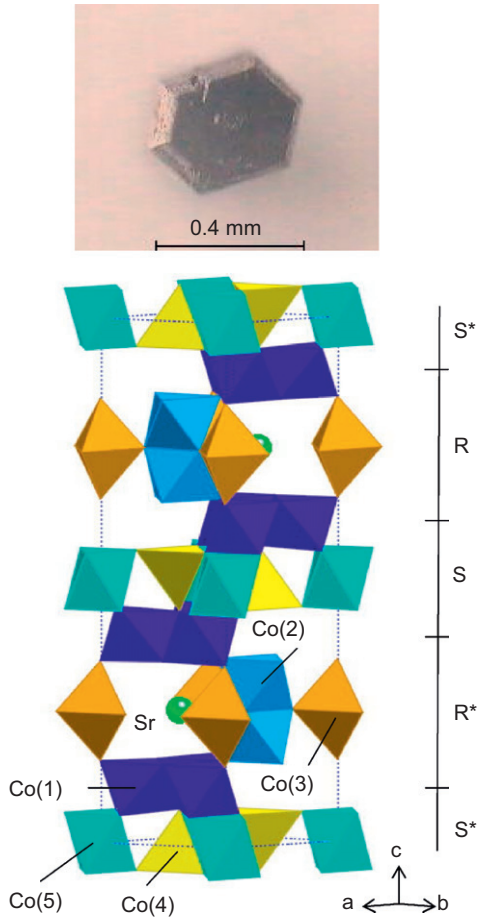

Fig. 1. (a) Magnified view of a single crystal of $SrCo_{12}O_{19}$. (b) Schematic crystal structure of $SrCo_{12}O_{19}$. The blocks of R* and S* are inverse to those of R (R-type hexagonal block; $SrCo_6O_{11}$) and S (spinel block; $2Co_3O_4$), respectively.

and 1000 °C for 0.5 h. After being taken out from the capsule, the product was washed with distilled water in an ultrasonic cleaner to remove NaCl, $SrCl_2$, and SrO. Synchrotron X-ray diffraction (SXRD) data of $SrCo_{12}O_{19}$ were collected on an imaging plate (IP) using a large Debye–Scherrer camera installed at BL02B2 of SPring-8, where the sample was sealed into a glass capillary with an internal diameter of 0.2 mm. The data collected in 0.01° step with the incident beam of a wavelength of 0.77596 Å were analyzed by the Rietveld method using a Rietan-2000 program [12].

The starting material for the crystal growth was an oxygen deficient Ruddlesden–Popper phase $Sr_3Co_2O_{7-\delta}$ ($\delta\sim1$) synthesized at 1050–1100 °C in air [13]. A mixture of $Sr_3Co_2O_{7-\delta}$ and KCl in a wt. ratio of 4:1 was sealed in a gold capsule ($\phi4\times6$ mm) and compressed at 3 GPa. The sample was heated to 800 °C at a rate of 80 K/min, then up to 950–1000 °C at a reduced rate of 2 K/min, and finally quenched to room temperature. As shown in Fig. 1(a), the single crystals of $SrCo_{12}O_{19}$ have a hexagonal morphology with a black luster ($0.35\times0.35\times0.2$ mm in dimension, typically). X-ray data for a single crystalline sample ($0.1\times0.1\times0.05$ mm in dimension) were collected on Rigaku R-AXIS RAPID using monochromated Mo$K\alpha$ radiation. Number of the reflections measured is 5860, and that of the independent reflections is 1512. The crystal structure was refined by the full-matrix least-squares on F technique. The occupancy factors were fixed at 1 during the final process because their deviations from 1 were negligible. DC magnetization was measured using single crystalline samples with a MPMS SQUID magnetometer (Quantum Design) in external magnetic fields of 1 and 7 T.

3. Results and discussion

3.1. Synthesis

The polycrystalline samples of $SrCo_{12}O_{19}$ were obtained by the following reaction:

$$12Na_{0.5}CoO_2 + 3SrCl_2 \xrightarrow{3\ \mathrm{GPa}\ 1000\ ^\circ\mathrm{C}} SrCo_{12}O_{19} + 6NaCl + 2SrO + 3/2O_2. \quad (1)$$

We regard this process as an exchange reaction driven by the great stability of NaCl. A powder X-ray diffraction pattern together with a calculated profile is shown in Fig. 2 (See the Supporting information for the refined structural parameters).

The crystal growth process of $SrCo_{12}O_{19}$ is essentially the same as that for $SrCo_6O_{11}$ in a sense that both crystals form from incongruently molten $Sr_3Co_2O_{7-\delta}$, though the pressure applied is slightly different as 3 GPa for $SrCo_{12}O_{19}$ and 2 GPa for $SrCo_6O_{11}$. The quenching from above the melting point (~950 °C), not slow cooling as for usual crystal growth, was needed to minimize the mixed formation of undesirable $[Sr_2O_{2-\delta}]_xCoO_2$ [14]. We note here that the Sr/Co ratio of the starting material $Sr_3Co_2O_{7-\delta}$ is deviated significantly from the target ratio. However, when the Sr/Co ratio was adjusted to $\frac{1}{12}$ by adding CoO, we could not obtain any single crystals, owing to an enhancement of the melting point. The excess SrO mixed with KCl is better flux for crystal growth.

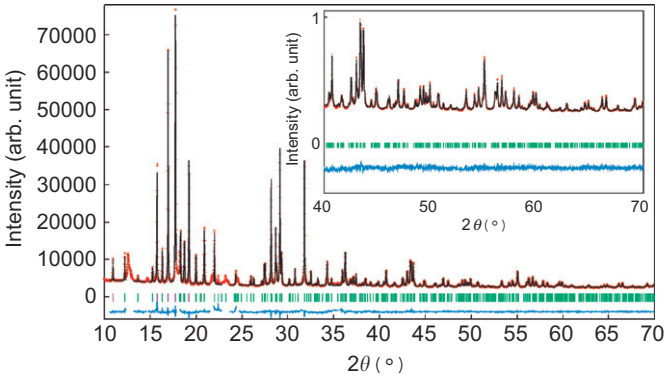

Fig. 2. Measured (+), calculated (line) and differential (bottom line) powder XRD patterns of $SrCo_{12}O_{19}$ ($\lambda=0.77596$ Å) taken at room temperature. The ticks indicate the positions of the reflections. Unidentified peaks from tiny amount of impurities were excluded during the refinements.

3.2. Structure

Structural analyses on the single crystalline sample showed $SrCo_{12}O_{19}$ to be isostructural with the M-type hexaferrite (S.G.: $P6_3/mmc$), as illustrated in Fig. 1(b). The refined structural parameters and the bond distances are given in Tables 1 and 2, respectively. The unit cell contains five different crystallographic sites for Co ions. The Co(1) ions are octahedrally coordinated, and these octahedral share their edges to form a Kagomé plane with a composition of $Co(1)_3O_8$. The Co(2) ions are also octahedrally coordinated, which are dimerized to $Co(2)_2O_9$ by face-sharing. The other Co ions form $Co(3)O_5$ trigonal bipyramids, $Co(4)O_4$ tetrahedra, and $Co(5)O_6$ octahedra (see Figs. 3(a) and (b)). The Sr ions are coordinated by 12 oxygen ions forming six relatively long Sr–O bonds (2.833 Å) within the mirror plane and six relatively short Sr–O bonds (2.643 Å) out of the mirror plane.

One of the important features of $SrCo_{12}O_{19}$, by contrast with $SrFe_{12}O_{19}$, is a wide charge distribution for Co ions over different crystallographic sites. Table 3 summarizes bond–valence calculations [15] using the refined Co–O bond lengths as $Co(1)^{3.50+}$, $Co(2)^{3.41+}$, $Co(3)^{2.76+}$, $Co(4)^{2.15+}$, $Co(5)^{3.49+}$ and also those for related cobalt oxides. Roughly mentioning, the tetrahedral site, Co(4), and the trigonal bipyramidal site, Co(3), have relatively low valences of +2 and +3, respectively, while those for the octahedral sites (Co(1), Co(2), Co(5)) are in between +3 and +4. It is worth noting that the tetrahedral site in Co_3O_4, a normal spinel, is occupied by a divalent Co ion, whereas that in the magnetite Fe_3O_4, an inverse spinel, is occupied by a trivalent Fe ion. Comparing $SrCo_{12}O_{19}$ with $SrCo_6O_{11}$, the valences of Co ions in the R-type block (Co(1)–(3)) are almost the same, though the averaged Co valence is significantly lower as $SrCo_{12}^{3+}O_{19}$ than that of $SrCo_6^{3.33+}O_{11}$. This is due to the presence of Co^{2+} at the tetrahedral site in the S-block of the former oxide.

Another point to be emphasized as an important feature of $SrCo_{12}O_{19}$ can be found at the trigonal bipyramidal site. It has been suggested by XRD analyses and Mössbauer studies that the potential within the trigonal bipyramid has double minima in M-type compounds such as $SrFe_{12}O_{19}$, $SrAl_{12}O_{19}$ and $SrGa_{12}O_{19}$ [16–18]. Although, in the single-crystal structure refinements of $SrCo_{12}O_{19}$, the least-square calculations assuming the two equivalent sites (4*e*) slightly away from the center of the trigonal bipyramid were less effective, the reminiscence of the double minima is reflected in the larger U_{33} values for Co(3) indicating an anharmonic thermal vibration of the atom (see Table 1).

3.3. Magnetism

Figs. 4(a) and (b) show the magnetism of $SrCo_{12}O_{19}$ measured in a magnetic field applied parallel (M_c/H) or perpendicular (M_{ab}/H) to the *c*-axis. At $H = 1$ T, two anomalies were found at low temperatures. At 80 K (T_{m1}), a sharp increase of M_{ab}/H sets in, indicating a long range magnetic ordering, whereas the corresponding anomaly for M_c/H is almost smeared out. The magnetic anisotropy becomes significant below T_{m1}. Around 5 K (T_{m2}), magnetization show a small downturn for either direction, which may presumably be caused by a spin reorientation. This downturn fades away at $H = 7$ T because the high-temperature spin structure is stabilized. The high-temperature magnetic susceptibilities can be fitted to a Curie–Weiss law, yielding Weiss temperatures of −57 and −47 K, respectively, indicating the predominance of antiferromagnetic interactions between the localized spins. The interpretation was reinforced by the

Table 2
Selected bond distances and bond–valence sums of cations for $SrCo_{12}O_{19}$

Atoms	Bond length (Å)	Atoms	Bond length (Å)
Co(1)–O(5) × 2	1.864(1)	Co(4)–O(4) × 3	1.913(1)
Co(1)–O(1)	1.907(1)	Co(4)–O(2)	1.948(2)
Co(1)–O(2)	1.923(1)		
Co(1)–O(4) × 2	1.923(1)	Co(5)–O(1) × 6	1.901(1)
Co(2)–O(3) × 3	1.903(1)	Sr–O(5) × 6	2.643(1)
Co(2)–O(5) × 3	1.915(1)	Sr–O(3) × 6	2.833(1)
Co(3)–O(3) × 3	1.846(2)		
Co(3)–O(1) × 2	2.107(2)		

Table 1
Refined positional and anisotropic thermal parameters (Å$^2 \times 10^4$) of $SrCo_{12}O_{19}$ single crystal with space group $P6_3/mmc$ (No.194)

Atom	Site	*x*	*y*	*z*	U_{11}	U_{22}	U_{33}	U_{12}	U_{13}	U_{23}
Sr(1)	2*d*	2/3	1/3	1/4	72.3(10)	U_{11}	56.3(13)	36.3(5)	0	0
Co(1)	12*k*	0.33266(4)	0.16632(2)	0.10834(1)	42.7(9)	43.4(6)	41.7(9)	21.6(4)	0.2(6)	0.3(3)
Co(2)	4*f*	1/3	2/3	0.19135(1)	45.8(10)	U_{11}	27.1(12)	23.2(5)	0	0
Co(3)	2*b*	0	0	1/4	56.7(12)	U_{11}	71.0(2)	27.9(6)	0	0
Co(4)	4*f*	1/3	2/3	0.02739(1)	67.9(10)	U_{11}	68.1(13)	34.3(5)	0	0
Co(5)	2*a*	0	0	0	48.3(12)	U_{11}	40(2)	23.9(6)	0	0
O(1)	4*e*	0	0	0.15392(6)	7(4)	U_{11}	64(7)	3(2)	0	0
O(2)	4*f*	2/3	1/3	0.06188(8)	72(5)	U_{11}	74(7)	36(2)	0	0
O(3)	6*h*	0.1876(1)	0.3753(2)	1/4	94(5)	28(7)	35(5)	14(3)	0	0
O(4)	12*k*	0.1486(1)	0.2972(2)	0.05604(5)	83(3)	79(5)	36(3)	40(2)	2.5(16)	5(3)
O(5)	12*k*	0.5070(1)	0.0140(2)	0.15223(5)	72(3)	89(4)	59(4)	45(2)	16(2)	32(3)

$a = 5.652(6)$ Å, $c = 21.81(2)$ Å, $V = 603.2(10)$ Å^3, $Z = 2$, $D = 6.049$ g/cm^3, $R = 5.49\%$, $R_W = 7.02\%$, Goodness of Fit Indicator = 1.009.

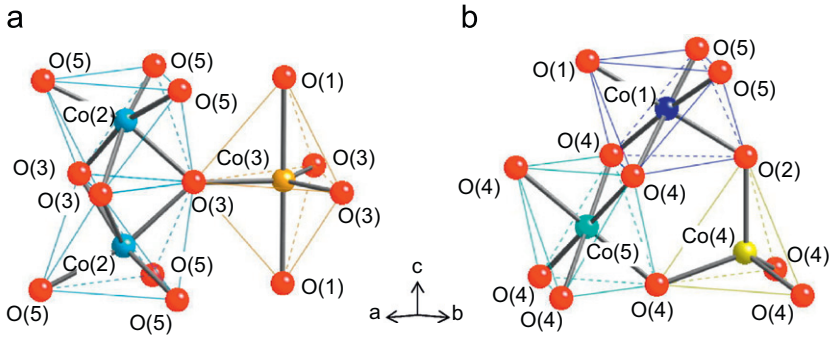

Fig. 3. (a) Magnified view of Co–O polyhedra located around $z = 0.25$, and (b) $z = 0$.

Table 3
Nominal valences and bond–valence sums (Σs_i) of Co ions in $SrCo_{12}O_{19}$, $SrCo_6O_{11}$, and Co_3O_4

Composition	Nominal Co valence	$Co(1)^{oct}$	$Co(2)^{oct}$	$Co(3)^{tri}$	$Co(4)^{tet}$	$Co(5)^{oct}$
$SrCo_{12}O_{19}$	+3	3.50	3.41	2.76	2.15	3.49
$SrCo_6O_{11}$	+3.33	3.56	3.44	2.78	–	–
Co_3O_4 (Ref. [26])	+2.67	3.28	–	–	2.11	3.28

The bond valence (s_i) is expressed as $s_i = \exp[(r_0 - r_i)/B]$; $B = 0.37$, $r_0 = 1.692$ for Co(4) and 1.70 for Co(1)–(3) and Co(5). The Co sites in $SrCo_6O_{11}$ and Co_3O_4 can be correlated with those in the R-type and S-type blocks of $SrCo_{12}O_{19}$, respectively. The nominal Co valences are calculated with assuming oxygen ions and barium ions are divalent. The superscripts on Co(1)–(5) represent oxygen coordinations; oct (octahedral), tri (trigonal bipyramidal), tet (tetrahedral).

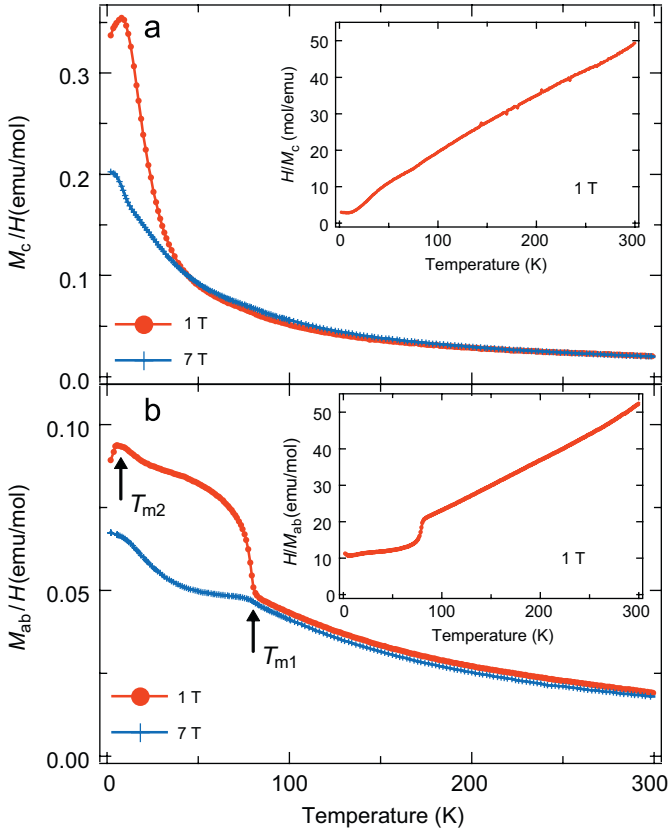

Fig. 4. Temperature dependence of molar magnetization divided by magnetic field for $SrCo_{12}O_{19}$, measured on heating after zero-field cooling (ZFC) in external magnetic fields of 1 and 7 T (a) parallel and (b) perpendicular to the c-axis. Inverse molar magnetic susceptibilities for both directions are shown as insets, respectively.

field-dependence of magnetization in the ordered states (Figs. 5(a) and (b)), that is, the magnetization was not saturated even at 7 T. At 50 K, both M_{ab} and M_c are linear against magnetic fields up to 7 T. On the other hand, as for the 2-K data, M_c shows metamagnetic behavior near 4 T and is much larger than the linear M_{ab}. Besides, small ferromagnetic hystereses were observed for both directions.

Next, we interpret the origin of magnetic behavior of $SrCo_{12}O_{19}$ by analogy to $SrCo_6O_{11}$. In the case of $SrCo_6O_{11}$, the trigonal bipyramidal site Co(3) has large localized moments with a uniaxial anisotropy as verified by NMR [19], neutron diffraction [20], and magnetization studies [9]. Lee et al. has proposed that a high-spin d^6 configuration $(xz/yz)^3(xy/(x^2-y^2))^2(z^2)^1$ $(S = 2)$ with a strong spin–orbit coupling under a uniaxial crystal field yields the uniaxial magnetic moments on Co(3) [21]. Considering the similarity between $SrCo_{12}O_{19}$ and $SrCo_6O_{11}$ in the local structures of the Co–O polyhedra, the bipyramidal site of $SrCo_{12}O_{19}$ is likely to have such a high-spin d^6 configuration with a strong uniaxial magnetic anisotropy and the octahedral sites are almost nonmagnetic. However, in order to fully understand the magnetic behavior, we have to consider the contributions from the other Co ions such as the tetrahedrally coordinated Co(4) ions. We suppose that these ions are in a d^7 configuration of $(x^2-y^2/z^2)^4(xy/yz/zx)^3$ $(S = \frac{3}{2})$, whose orbital moment is essentially absent and, therefore, magnetic contribution is isotropic.

Cobalt oxides show a rich variety of magnetic properties inherent to their various electronic configurations coupled to the crystal structures: (i) perovskite-related phases, Sr_nCo_{n-1}

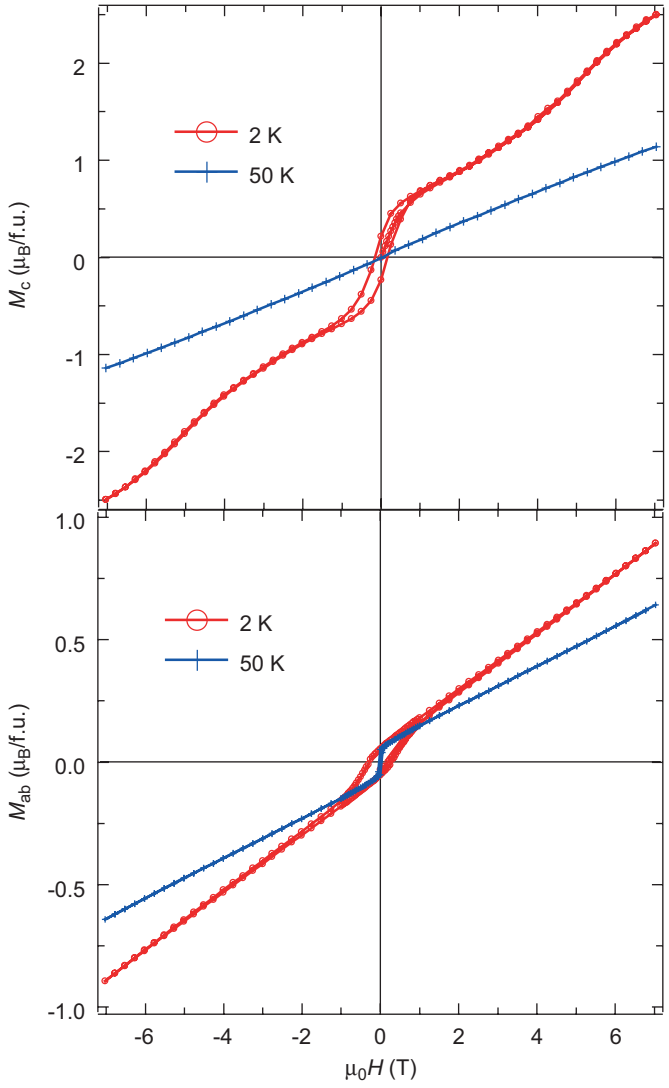

Fig. 5. Magnetization curves of $SrCo_{12}O_{19}$ at 2 and 50 K measured with an external magnetic field parallel (a) and perpendicular (b) to the c-axis.

O_{3n-2} ($n = 2$, 3, 4, and ∞) [22,23] showing ferromagnetism with rather high Curie temperatures; (ii) pseudo-one-dimensional hexagonal compounds $(A_3Co_2O_6)_n(A_3Co_3O_9)_m$ (A = Ca, Sr) [24] showing geometrically frustrated magnetism exemplified by a $\frac{1}{3}$ magnetization plateau in $Ca_3Co_2O_6$ [25]. Additionally to them, hexaferrite-type cobalt oxides $(SrCo_6O_{11})(Co_3O_4)_{2n}$ ($n = 0,1$) found at HPs of several GPa will be a new class of interesting magnetic systems dominated by the Ising-like spins at the trigonal bipyramidal site.

4. Conclusions

A new magnetoplumbite-type hexagonal cobalt oxide, $SrCo_{12}O_{19}$, has been synthesized under a HP of 3 GPa. We have performed X-ray structure analyses using the single crystal of $SrCo_{12}O_{19}$ and found that, based on bond–valence calculations, valences of five kinds of Co ions are distributed widely from +2.15 to +3.5. Magnetic susceptibilities showed magnetic transitions at T_{m1}, where a long range magnetic ordering sets in, and at T_{m2}, below which the magnetization along the c-axis becomes non-linear. Although it is not easy to give a straightforward explanation for the magnetic ground state of $SrCo_{12}O_{19}$ due to the multiplicity of magnetic sites, we have attributed a major role in the anisotropic magnetism to the trigonal bipyramidal site Co(3), on analogy to $SrCo_6O_{11}$.

Acknowledgments

The authors thank T. Saito and T. Katsufuji for useful comments. The synchrotron radiation experiments were performed at the SPring-8 with the approval of the Japan Synchrotron Radiation Research Institute. This work was supported by the Ministry of Education, Culture, Sports, Science and Technology, Japan Grants-in-Aid no. 17105002. S. I. receives additional support from JSPS.

Appendix A. Supporting information

Supplementary data associated with this article can be found in the online version at doi:10.1016/j.jssc.2008.02.024.

References

[1] H. Kojima, in: E.P. Wohlfarth (Ed.), Ferromagnetic Materials, Vol. 3, Amsterdam, North-Holland, 1982, pp. 305–391.
[2] H. Pfeiffer, R.W. Chantrell, P. Gornert, W. Schuppel, E. Sinn, M. Rosler, J. Magn. Magn. Mater. 125 (1993) 373–376.
[3] A.M. Srivastava, W.W. Beers, J. Lumin. 71 (1997) 285–290.
[4] X. Obradors, A. Labarta, A. Isalgué, J. Tejada, J. Rodriguez, M. Pernet, Sol. St. Commun. 65 (1988) 189–192.
[5] P.E.D. Morgan, J.A. Miles, J. Am. Ceram. Soc. 69 (1986) C157–C159.
[6] O. Kubo, T. Ido, H. Yokoyama, IEEE Trans. Magn. 18 (1982) 1122–1124.
[7] X. Batlle, X. Obradors, J. Rodriguez, M. Pernet, M.V. Cabañas, M. Vallet, J. Appl. Phys. 70 (1991) 1614–1623.
[8] X. Batlle, A. Labarta, B. Martínez, X. Obradors, V. Cabañas, M. Vallet-Regí, J. Appl. Phys. 70 (1991) 6172–6174.
[9] S. Ishiwata, D. Wang, T. Saito, M. Takano, Chem. Mater. 17 (2005) 2789–2791.
[10] S. Ishiwata, M. Lee, Y. Onose, N.P. Ong, M. Takano, I. Terasaki, J. Magn. Magn. Mater. 310 (2007) 1989–1990.
[11] S. Ishiwata, I. Terasaki, F. Ishii, N. Nagaosa, H. Mukuda, Y. Kitaoka, T. Saito, M. Takano, Phys. Rev. Lett. 98 (2007) 217201, (4p).
[12] F. Izumi, T. Ikeda, Mater. Sci. Forum 198 (2000) 321–324.
[13] S.E. Dann, M.T. Weller, J. Solid State Chem. 115 (1995) 499–507.
[14] S. Ishiwata, I. Terasaki, Y. Kusano, M. Takano, J. Phys. Soc. Jpn. 75 (2006) 104716, (4p).
[15] N.E. Brese, M. O'Keeffe, Acta Crystallogr. Sect. B 47 (1991) 192–197.
[16] X. Obradors, A. Collomb, M. Pernet, D. Samaras, J.C. Joubert, J. Solid State Chem. 56 (1985) 171–181.
[17] K. Kimura, M. Ohgaki, K. Tanaka, H. Morikawa, F. Marumo, J. Solid State Chem. 87 (1990) 186–194.
[18] E. Kreber, V. Gonser, A. Trautwein, F. Harris, J. Phys. Chem. Solids 36 (1975) 263–265.
[19] H. Mukuda, Y. Kitaoka, S. Ishiwata, T. Saito, Y. Shimakawa, H. Harima, M. Takano, J. Phys. Soc. Jpn. 75 (2006) 094715, (5p).

[20] T. Saito, A. Williams, J.P. Attfield, T. Wuernisha, T. Kamiyama, S. Ishiwata, Y. Takeda, Y. Shimakawa, M. Takano, J. Magn. Magn. Mater. 310 (2007) 1584–1586.
[21] C. Lee, M.-H. Whangbo, A. Villesuzanne, Chem. Mater. 19 (2007) 2712–2714.
[22] J. Matsuno, Y. Okimoto, Z. Fang, X.Z. Yu, Y. Matsui, N. Nagaosa, M. Kawasaki, Y. Tokura, Phys. Rev. Lett. 93 (2004) 167202, (4p).
[23] X.L. Wang, H. Sakurai, E. Takayama-Muromachi, J. Appl. Phys. 97 (2005) 10M519, (3p).
[24] K. Boulahya, M. Parras, J.M. Gonza′lez-Calbet, Chem. Mater. 12 (2000) 25–32.
[25] H. Kageyama, K. Yoshimura, K. Kosuge, H. Mitamura, T. Goto, J. Phys. Soc. Jpn. 66 (1997) 1607–1610.
[26] X. Liu, C.T. Prewitt, Phys. Chem. Miner. 17 (1990) 168–172.